Mid-Semester Report

The Art of Scientific Computing: Investigating the Mass of the Neutrino

Author:
Kyla Adams

Subject Handbook code:
COMP-90072

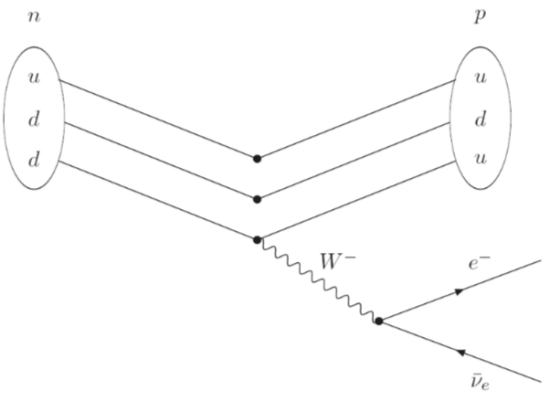

Faculty of Science
The University of Melbourne

26th April 2018

Subject co-ordinators: A/Prof. Roger Rassool & Prof. Harry Quiney

Tutor: Innes Bigaran

Contents

Chapter 1

Introduction to the Standard Model

The Standard Model is the theory used to describe the fundamental particles and their interactions. However, the theory has its shortfalls, such as the inability to reconcile gravity within the model, and the presence of dark matter in the universe. Another large gap still to be filled is the measured mass of the neutrino. Theory initially suggested that the neutrino may not even be able to be observed (Bethe and Peierls 1934). In 1998 neutrino oscillations were measured for the first time. Since then, many experiments being conducted around the world are working to measure this mass. Some of these experiments have lead to Nobel Prizes (Takaaki Kajita and Arthur B. McDonald in 2015), as a consequence of neutrino oscillations. Many of these experiments would not have been able to gain funding if they were not already very confident in the ability of the machinery to physically make a detection. In order to gain this confidence many smaller scale experiments and computer simulations would have been run. This project will detail just some of these many calculations and show how they can be important in gaining funding and paving the way to Nobel prize worthy discoveries. Through the use of a jupyter notebook (available at *GitHub*) the different methods and some of the computational methods are explained. The notebook is able to be completed independently of this report, however, a fuller understanding will be gained by reading them both in tandem.

1.1 Background

The Standard Model has a long history in physics. The first elementary particle to be discovered was the electron in 1897, which started the chase towards finding the other particles and the nature of the fundamental forces that govern everyday life. Over the years, the picture was slowly filled in by many scientists until it became what it is today. The Standard Model (see Figure 1.2) is separated into 3 groups; leptons, quarks and bosons. These groups are further separated into flavours. Each of these neutrino flavours have different abundances in the universe and they all mix via a process called quantum mechanical oscillations (commonly called neutrino oscillations). The exact mixing process is beyond the scope of this report, however the knowledge that the neutrino flavours can mix is important. The electron neutrino mass is the mass of interest here, however in some calculations it is only possible (at this level) to determine the mass of all the neutrino flavours. For this reason, sometimes the resultant neutrino mass calculation is $m_\nu = \frac{1}{3}\sum_j m_j$. In all fundamental particle interactions energy is always conserved. The Feynman diagram seen in Figure 1.1 shows a neutron decaying to a proton, electron and neutrino. By charge conservation, the down quark converts to an up quark via a W^- boson. The boson then decays to the electron and neutrino.

The mass of the neutrino can be determined through experimental methods as well as computational simulation. This report investigates these methods and the limits that they can place on future measurements.

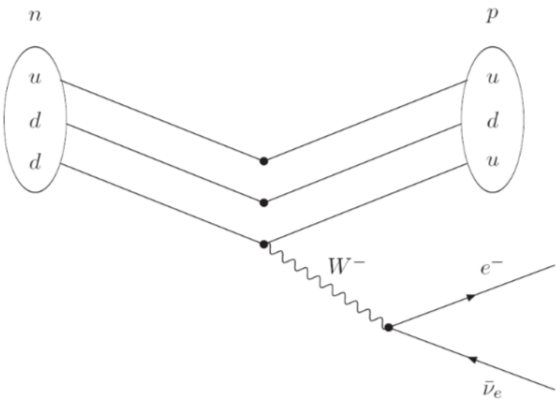

Figure 1.1: The Feynman diagram of a beta decay. Up quarks have a charge of $+\frac{2}{3}$, down quarks have a charge of $-\frac{1}{3}$, as the neutron decays to a proton, charge conservation means that an electron and a neutrino must be emitted

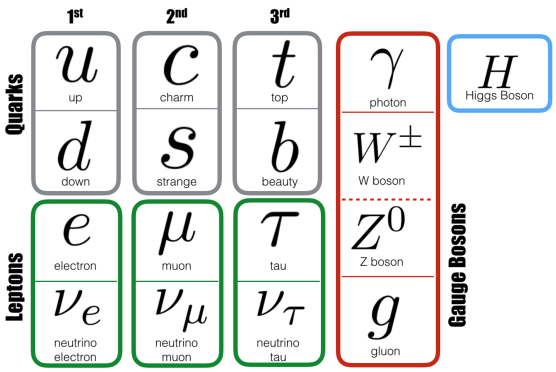

Figure 1.2: The Standard Model (University of Zurich, 2018). The three groups shown are, leptons, quarks and bosons and each are separated into their flavour groups (numbered 1 to 3 from left to right). The neutrino is a lepton and it's first flavour will be investigated here (the electron neutrino) (University of Zurich, 2018).

Chapter 2

Neutrino single β Decay

Neutrinos were first theorised to exist by Wolfgang Pauli in 1930. Over the next couple of years many scientists became convinced that the neutrino must exist in order to maintain the conservation of energy and angular momentum (Bethe and Peierls 1934).The hypothesis of the existence of neutrinos arose due to defects in two theories surrounding the existence of protons and neutrons. These problems were, the appearance of a continuous energy spectra in beta decay and the presence of spin in some the nuclei (Bilenky 2013). In 1934, Enrico Fermi further contributed to the possible existence of the neutrino in the context of the theory of Beta decay. By 1954 an experiment was proposed and run in order to attempt to detect the particle. The neutrino was first detected by Reines and Cowan 1959 by measuring the cross section of positron decay. Since then, the measurement of the energy spectra from beta decay of a known source has been used to place some limits on the mass of the neutrino.

2.1 Beta Decay

Beta decay is the process of a proton (or neutron) decaying to an electron (or positron) and a neutrino. These processes are outlined below:

$$p \rightarrow n + e^{+} + \nu_e \,, \tag{2.1}$$

$$n \rightarrow p + e^{-} + \bar{\nu}_e \,, \tag{2.2}$$

where p and n are the proton and neutron, e^{+} and e^{-} are the positron and electron and ν_e is the electron neutrino. The emission of the neutrino is inferred from the conservation of energy. In the beta decay of a neutron, the resulting electron was expected to have a fixed kinetic energy equal to the energy of neutron minus the energy lost in the conversion. When the energies from this process were recorded, instead of a distinct spike in the kinetic energy, a continuous spectrum was observed with an end point around, but less than, the total energy released. The neutrino was the source of the continuous spectrum, however the deficit on the energy spectrum was still unexpected. In the rest frame of the parent nucleus the daughter particles are emitted with no recoil. This results in a transfer of kinetic energy. If there were no neutrino, the kinetic energy would be larger than if there is one present. The energy defect can be determined to be

$$Q = T_e + E \,,$$

where E is the energy of the system and $T_e = E_e - m_e$ is the kinetic energy of the electron. The neutrino mass m_ν can be inferred from the momentum of the neutrino

$$p_\nu = \sqrt{(Q - T_e)^2 - m_\nu^2} \,.$$

Determining the mass of the neutrino has been the aim of many experiments across the world; KATRIN, Project 8, ECHo and HOLMES are just some the examples (Palanque-Delabrouille et al. 2015). These experiments have been run using a variety of different methods. Some cosmological methods have been utilised to set limits on the neutrino mass to be < 120 MeV (Palanque-Delabrouille et al. 2015; Zennaro et al. 2018; Huang, Ohlsson, and Zhou 2018). Other limits have been made by using terrestrial means such as Neutrino beams and high energy colliders (ArgoNeuT Collaboration et al. 2018). These methods have been designed to have a sensitivity of ~ 200 MeV (HyperKamiokande, DUNE etc). The actual mass of the neutrino is still to be determined. However these limits allow for the reduction of the parameter space allowed for the mass which will eventually lead to stringent limits on the mass of the neutrino.

The measurement of the mass of the neutrino mass from beta decay can easily be recreated in a university physics lab. This is achieved through the knowledge of kinematics. As the parent nucleus decays to the daughter an electron (or a positron) and a neutrino are emitted (Mertens 2016). The energy required for the decay is imparted to both the electron and the neutrino. The experimental setup can be seen in Figure 2.1. A Pm^{147} source placed on the edge of the system. This source undergoes beta decay. As the decaying particles are emitted from the source they are exposed to a magnetic field. This field causes the electrons to curve and interact with an electron detector that then measures the energy of the electron. The magnetic field can be manipulated so that the electron will travel along a certain radius. From these values the kinetic energy of the electron can be determined. The kinetic energy of the electron can be determined by:

$$T = E - m_e c^2 \,, \tag{2.3}$$

where E is the measured energy, m_e is the mass of the electron and c is the speed of light. In particle physics the maths becomes simple when everything is in natural units. Table 3.1 shows the constant values used throughout.

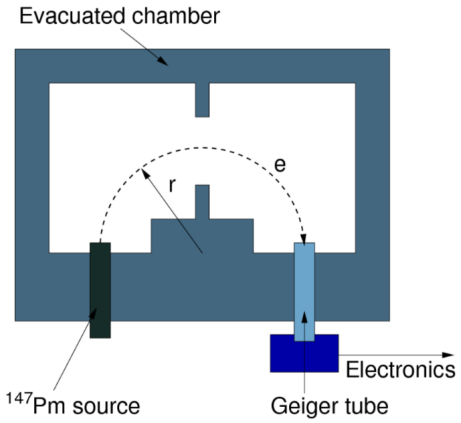

Figure 2.1: Experimental Setup for the measurement of the beta decay of a Pm^{147} source. radioactive source is placed in a vacuum chamber with a magnetic field present. The electrons emitted from the decay are trapped in the field and directed to a detector where their energies are recorded.

In addition to the conservation of charge, the conservation of energy must also be followed. The energies of the initial and final states in the beta decay should equal the energy of the emitted particles:

$$E_0 = E_{initial} - E_{final} \tag{2.4}$$

The 'endpoint' energy can then be utilised to infer the energy that was carried away from the emitted neutrino which cannot be directly measured in this setup. This energy, when experimentally determined by Geoppert-Mayer in 1935 determined that the electrons had an energy difference less than expected along a continuous spectrum.
Many different radioactive materials can be used in this experiment. However, those with short half lives and a lower endpoint in the energy maximises the area of the energy spectrum of interest (the linear decay region). In addition a source that has a good resolution in the experimental sampling range of $\sim 2eV$ is needed. If a larger sampling range is used then some fundamental physics could be missed within the band gaps. A larger sampling range would change the validity of the Kurie plots as they rely on the distinct relation between the energy measured and the detected values.

2.2 Kurie Plots

From the determination of the endpoint in the energy spectrum and the assumption that in the beta decay the electron is emitted with a certain momentum, the final momentum imparted to the neutrino can be determined:

$$p_f = \frac{16\pi^2}{h^6 c^3} p^2 (T - E_0) dp \,, \tag{2.5}$$

where T is the kinetic energy of the electron. Once the momentum of the final states is determined, through the use of Fermi's Golden rule,

$$\omega(p)dp = \frac{4\pi^2}{c} |M_{if}|^2 p_f \,. \tag{2.6}$$

The Golden rule states the probability that an electron will have a certain momentum p at a time ω, here M_{if} is a matrix element taken from Quantum Field Theory and will not be calculated. Instead from this momentum probability a new variable can be defined that can be determined from the experimental data. This variable is called the Kurie Variable. It is defined by substituting Equation 2.5 into Equation 2.6. Then by setting the Kurie Variable to be equal to the square root of the momentum probability divided by p^2 the following can be determined:

$$K(Z,p) = \sqrt{\frac{\omega(p)}{p^2}} \tag{2.7}$$

$$= \frac{8\pi}{h^{7/2}c^{3/2}}|M_{if}|(T - E_0) \tag{2.8}$$

By assuming that the matrix element is approximately constant the linear region of the plot of the energies against the Kurie variable will produce a value for E_0.
Experimentally, the momentum probability is equivalent to the energy distribution of the electron counts. Chapter 3 explores the experimental data and the validity of the assumptions that lead to the conclusion stated above.

Chapter 3

Data Analysis

Utilising the experimental setup described in 2, the data was collected and stored in the data file *Experimental_Data*. The columns of the file are:

- [0] Current: measured in mA
- [1] Current uncertainty of $\pm 2mA$
- [2] Counts: number of decays measured in 100s
- [3] Corrected Counts: a number of counts in lag between detection
- [4] B: mag field in Tesla (calculated from current)
- [5] B uncertainty from current
- [6] p: momentum in $kg.m.s^{-1}$
- [7] E_{TOT} in keV
- [8] E_{TOT} in J
- [9] T: kinetic energy
- [10] Kurie variable: calculated from counts and momentum

Throughout the project, python3 was used to write and import code. This code can be found in the attached file and displayed as a *jupyter notebook* (Also see *GitHub* for the repository and full code). Figure 3.1 shows the very basic structure of the code. Different colours represent different code structures. The arrows can be read as is called in, ie the Function **import_data** *is called in* **LineFit**.

Initially a program **import_data** was written that imports the data file from the folder **data_files** as a *pandas* data set. This program was then called in all other relevant scripts where the data was needed. Table 3.1 shows the constant values used throughout the project.
The first step in analysing the data was to generate a plot of the kinetic energy against the Kurie Variable.This allowed for a check of the given data. The kinetic energy was determined from the Energy in keV $T = E - m_e c^2$ using the mass of the electron in natural units (See Table 3.1 for a list of relevant constants). Figure 3.2 shows the plot, there is a distinctive linear region that will be examined and used to generate the Kurie plot.

The next step was to generate the Kurie plot of the data. This was done by approximating the boundaries on Figure 3.2 where the data was linear. These boundaries were chosen to be between 90 keV and 190 keV. Figure 3.2 shows these boundaries and Figure 3.3 shows the resulting Kurie Plot. The data can be fit using a linear least squares line fitting algorithm. This method minimised the estimated parameters using the given data. The least squares fitting method works by taking an initial 'guess' for the gradient then determines the validity of the fit by comparing it to the gradient of the data set. If the value is determined not to be a good fit, the process is repeated. Otherwise the final gradient and intercept are printed along with their associated error.

The python script *LineFit* was used to determine the values for the linear line that minimise the difference from the experimental variables and determines the standard deviation from the data. The function *plot()* in the *LineFit* code gives the options to plot the data on it's own, with the linear fit or with the linear fit and errors, See Appendix B for a section of the line fitting code (Figure B.1). The code sample below shows this function. The

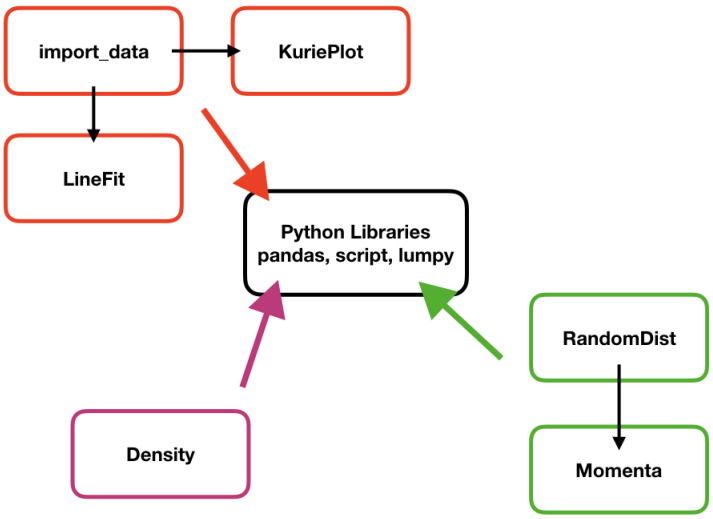

Figure 3.1: The top level structure of the project code

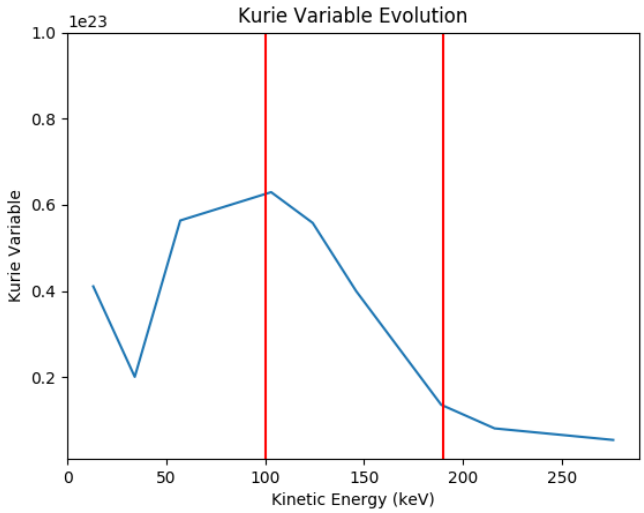

Figure 3.2: The region of linearity outlined to be used in the Kurie Plot

options are given to make the code more user friendly and allow the user to only plot the desired variables.

From the linear fit the intercept of the date (E_0) was found to be $1.262 \times 10^{23} \pm 10^{10}$. This is the initial energy of the decay system. From this an upper limit on the mass of the neutrino can be determined. These limits on the neutrino mass are very large. A small scale experiment such as this can be very difficult to produce accurate measurements, due to the limited sample size and large uncertainties in generating values. Despite this, experiments are necessary to start placing smaller limits through other experiments.

description		**value**		
electronic charge	e	1.6×10^{-19}C		
proton mass	m_p	938MeV/c^2		
electron mass	m_e	511keV/c^2		
speed of light in vacuum	c	$2.9979246 \times 10^{+8}$ m/s		
Planck constant	h	$6.6260696 \times 10^{-34}$ J$\cdot$s	or	$4.1356675 \times 10^{-15}eV\cdot$s
reduced Planck constant	$\hbar$	$1.0545717 \times 10^{-34}$ J$\cdot$s	or	$6.5821193 \times 10^{-16}eV\cdot$s

Table 3.1: A table of measured constants.

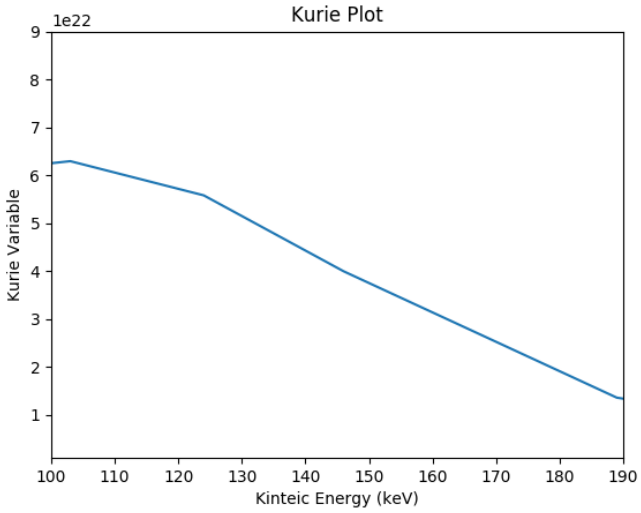

Figure 3.3: The Kurie plot of the generated data.

3.1 Neutrino Beam Experiments

Neutrino beams are one of the many experimental methods utilised in the attempt to determine the mass of the neutrino. Neutrino beams use collimated beams of fundamental particles, such as pions, and measure their decay. Pions and Kaons decay into neutrinos and muons:

$$\pi^+ \rightarrow \mu^+ + \nu_\mu \,, \tag{3.1}$$

$$K^+ \rightarrow \mu^+ + \nu_\mu \,. \tag{3.2}$$

These decay process happen with a probability of 1.00 and 0.64 respectively. The products of the decay will have arbitrary momenta and direction. The neutrinos are what are desired, therefore their directional decay needs to be controlled as much as possible. In a simplified simulation, this is achieved by starting with a beam of a mixture of pions and kaons. As these particles decay the products are passed through a magnetic horn that sends the muons on a different path to the neutrinos. If the initial beam is very collimated then the resulting neutrinos will also be collimated due to the conservation of momentum, however the neutrino beam profile will be larger than the initial profile. The resulting neutrino beam is incident on a detector where measurements are made.
Both pions and kaons are highly relativistic. As a result calculations and measurements need to be adjusted. The decay time for a meson is:

$$f(t) = \frac{1}{\tau_0} e^{-\frac{t}{\tau_0}} \,, \tag{3.3}$$

. where τ_0 is the decay time of the particle in its rest frame. The distance that a particle will travel in the laboratory frame is determined by:

$$s = \frac{p}{m} ct \,, \tag{3.4}$$

where p is the particle momentum, m is the particles mass, c is 3×10^8 m/s and t is the time in seconds. In order to determine the distance travelled, the particle will travel in the laboratory frame the momentum needs to be adjusted, this is done through a Lorentz transformation. If the mass of the neutrino is assumed to be fixed, the magnitude of its momentum can be determined by:

$$|p_\nu| = \frac{m_\pi^2 + m_\mu^2}{2m_\pi} \,. \tag{3.5}$$

Once the momentum is known, the scattering angle of the neutrinos can be found. This is achieved by simulating the transverse and longitudinal components of the momenta and shifting them into the lab frame. A normal distribution of angles between -1 and 1 are generated. The longitudinal and transverse momenta are then determined by:

$$p_l = |p_\nu| \cos(\theta) \,, \tag{3.6}$$

$$p_t = |p_\nu| \sin(\theta) \,. \tag{3.7}$$

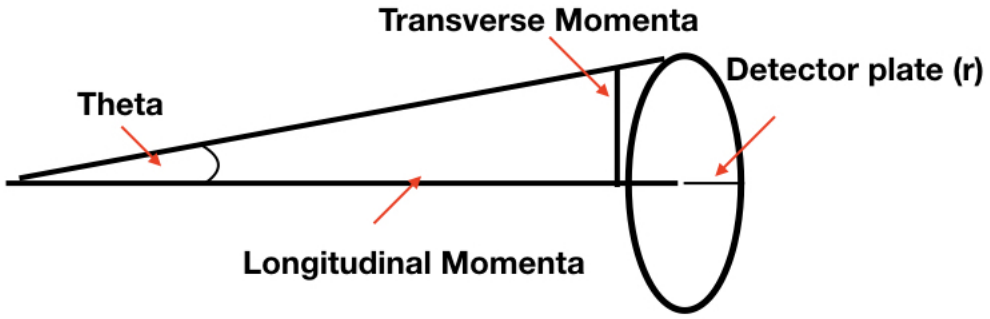

Figure 3.4: Schematic of the momenta components of a neutrino beam experiment

A lorentz transformation is then applied.

$$\begin{pmatrix} p_l \\ p_t \\ |p| \end{pmatrix}_{lab} = \begin{pmatrix} \gamma & 0 & \beta \times \gamma \\ 0 & 1 & 0 \\ \beta \times \gamma & 0 & \gamma \end{pmatrix} \begin{pmatrix} p_l \\ p_t \\ |p| \end{pmatrix}_{rest} , \tag{3.8}$$

where β is:

$$\beta \frac{|p_{meson}|}{\sqrt{p_{meson}^2 + m_{meson}^2}} . \tag{3.9}$$

Figure 3.4 shows a schematic diagram of the different momenta components. It shows a cross section of the neutrino beam with the mesons travelling from the left to right on the horizontal axis. In order to simulate a neutrino beam, a distribution of random numbers needs to be generated. These distributions are never truly random. To generate a distribution an algorithm is applied to a random number and is then used to determine what the next value will be. This process is called a Monte Carlo simulation. There are two main different types of distributions that are generated through this process, normal and uniform. Normal distributions are also informally referred to a bell curves. These distributions have the form

$$f(x) = \frac{1}{\sqrt{2\pi} e^{\frac{-}{(x-\mu)^2} 2\sigma^2}} ,$$

where μ is the mean and σ is the standard deviation. Non uniform distributions are distributions where the probability becomes weighted in someway towards certain values. A non-uniform distribution can be generated from a uniform distribution. In addition to these classifications, the numbers can further be categorised into continuous and discrete values. A continuous distribution allows for all possible values within a specified range, whereas a discrete distribution will only give the integer values. These categories can effect the probabilities of certain values in different ways to a continuous one. In the case of modelling the meson decays, a continuous distribution is useful. The momenta and angles simulated are not discrete, however, other cases such as simulating the percentage of particles that hit a detector can be modelled by a discrete distribution.

Figure 3.6 shows the flowchart of the code implemented to model a uniform distribution of values between 0 and 1 that are then transformed according to a non-uniform distribution to model the expected momenta values of the initial mesons present in a beam experiment. This is achieved through the use of the 'Accept-Reject' method. A random variable x is generated, a new variable u is then calculated such that $u = 2x - 1$. This is repeated for two different x values. A variable u is then calculated by $d^2 = x_1^2 + x_2^2$. The if statement outlined in the flowchart is then performed. The y value is then calculated with the u values such that $y = u\sqrt{-2ln(d)/d}$ This process is repeated for as many random numbers as desired. After this the random distribution can be transformed to a desired mean and standard deviation such that $z = mean + std * y$. The resulting momenta distribution can be seen in Figure 3.5

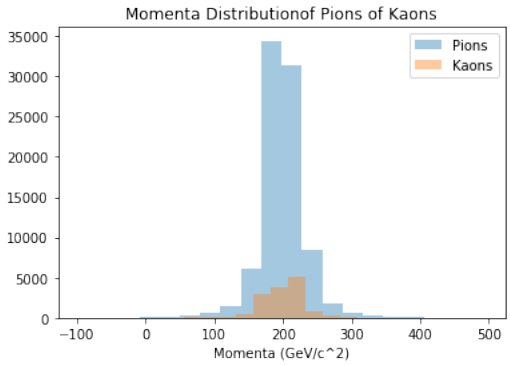

Figure 3.5: A shifted normalised distribution of momenta with mean of 200Gev and standard deviation of 10Gev

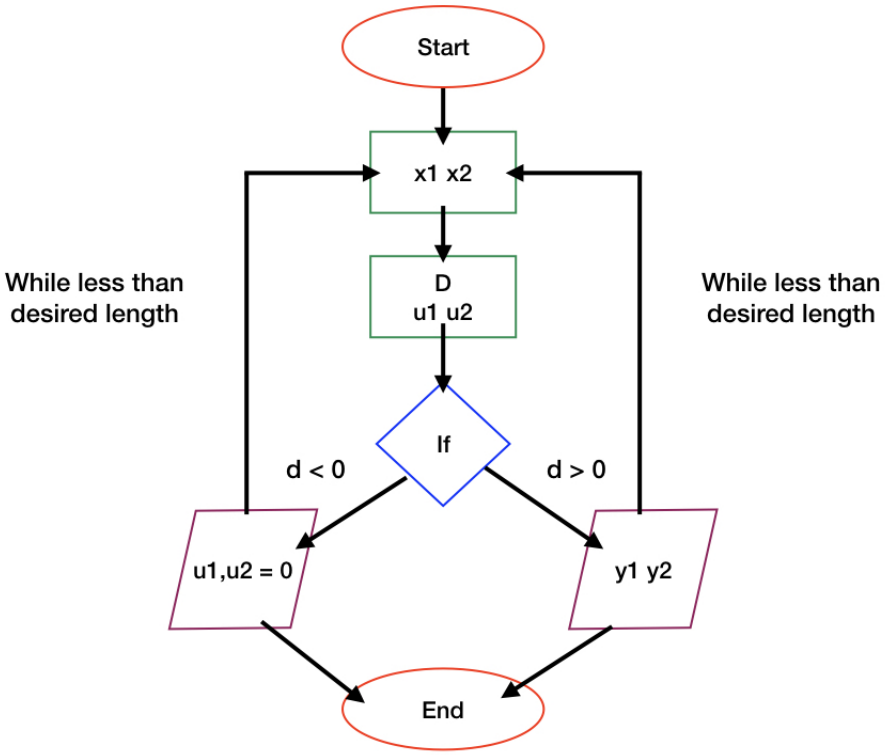

Figure 3.6: Coding flow chart depicting the generation of a distribution of random numbers. The methods used to initialise the variables are stated in the body of the work

The initial momenta distributions of both the pions and kaons can be seen in Figure 3.5. From these momenta the decay distance of the mesons is determined using

$$s = \frac{p}{m}\tau c \, .$$

The differences between the distributions is due to the different lifetimes of the mesons. The kaon has half the lifetime of the pion and therefore it's distances are significantly shorter. This means that the neutrinos generated from the decay of a kaon will appear sooner in the experimental tunnel than the pions. This will result in them having a larger spread at the detector plate than the other neutrinos. The decay distances can be found after performing the Lorentz transform and can be seen in Figure 3.7.

From the decay distances of the mesons, the decay distance of the neutrinos can be determined. If the length of the tunnel is 1000 m and the pions decay at 700 m then the neutrino distance is

$$|s - 700| \sin\theta < 1.5 \, .$$

The angle $\sin(\theta)$ can be found by $\frac{p_{t,lab}}{E_{\nu,lab}}$. If the condition above is met then the emitted neutrinos will hit the detector plate. These momenta have been separated into their transverse and longitudinal components. This

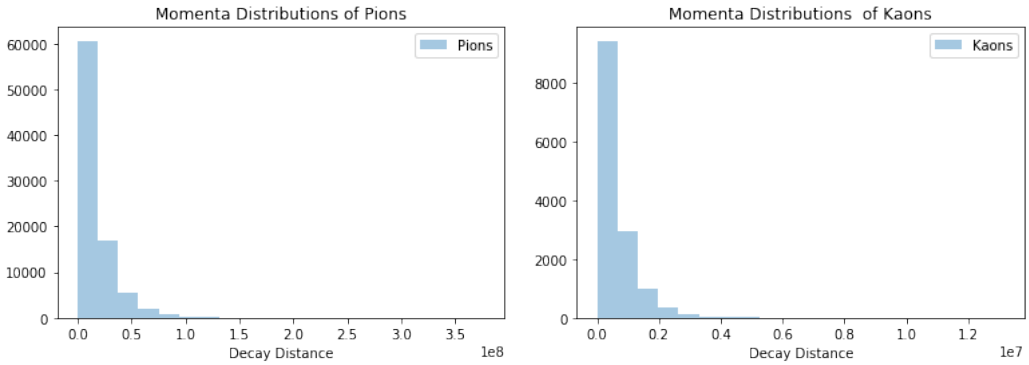

Figure 3.7: The calculated decay distances in the laboratory frame

is necessary as once the mesons have decayed the resultant neutrinos will be travelling at an angle to the horizontal. This introduction of the transverse momenta means that some of the neutrinos may not hit the detector plate (with radius 1.5m).

In this simulation, the majority of the neutrinos from both the pion and kaon decays hit the detector plate. This allows for a measurement of the mass of the neutrino. The energies of the resultant neutrinos can be calculated from these detector plates. In addition, the position of the neutrino from the centre of the plate can also give an indication of the neutrino mass. The more energetic the neutrino, the further from the plate it will be found.

Chapter 4

Cosmology

The study of cosmology is one of the fields where particle physicists and astrophysicists works closely together. Through the study of the cosmos, limitations upon the neutrino mass can be determined. The big bang was a highly ionising event. Fundamental particles were interacting constantly resulting in the emission of photons and neutrons. These photons have resulted in an almost uniform distribution across the universe, the Cosmic Microwave Background. This period of time in the universe is known as Big Bang nucleosynthesis. During this time the decay of various particles resulted in the emission of photons and neutrinos Huang, Ohlsson, and Zhou 2018. The CMB consists of a photon relic density, as well as a neutrino relic density. This density can be used to determine limits on the neutrino mass.

The time evolution of the universe is governed by the Friedmann Equations:

$$H^2 = \frac{8\pi G}{3c^2}\rho \,, \tag{4.1}$$

where $H = \frac{\frac{da}{dt}}{a}$, ρ is the total energy density and $a = a(t)$ is the scale factor of the universe ($a = 1$ today). The total energy density of the universe is constantly evolving with time. the rate of this evolution is dependant on the presence of dark matter and what energy is dominate at stages of the galaxy (such as radiation). The total density is defined as the sum of all the constituent particles in the universe ie $\rho = \rho_e + \rho_\gamma + \rho_\nu + ...$ The density of any particular particle (X) relative to the number of photons present can be determined,

$$r_X = \frac{n_X}{n_\gamma} \,.$$

This fraction evolves with time as:

$$\frac{dr_X}{dt} = -\beta_X n_\gamma \left(r_X^2 - r_{X,eq}^2\right) \,,$$

where $r_{X,eq}$ is the number density of the particle X in equilibrium and $\beta_X n_X^2$ is the annihilation rate of particle X. In the case of neutrinos the annihilation process is $\nu + \bar{\nu} \rightarrow y\bar{y}$ where y is a particle slightly lighter than the neutrino. This results in a β_ν value of $\sim G_F^2 m^2$ where G_F is the Fermi constant (290 $GeV)^-2$. By using these equations the equilibrium density of neutrinos can be determined. Once the equilibrium density is found the neutrino masses can be determined through the use of a density function.
The equilibrium density of the neutrinos present in the universe can aid in determining their masses. This density can be found by:

$$n_{\nu,eq} = \frac{g_\nu}{8\pi^3}\int f(p) d^3p \,, \tag{4.2}$$

$$= 4\pi \frac{g_\nu}{8\pi^3}(p) d^2p \,, \tag{4.3}$$

where the function for a fermion species is:

$$f(p) = \frac{1}{e^{(p-\mu_\nu)/T} - 1} \,, \tag{4.4}$$

where μ_ν is the chemical potential of the neutrino. By integrating equation 4.3 for a variety of chosen temperatures. In order to do this $g_\nu = 4$ and μ_ν was assumed to be small. For the equilibrium density of photons take $n_{\gamma,eq} = 410 cm^3$.

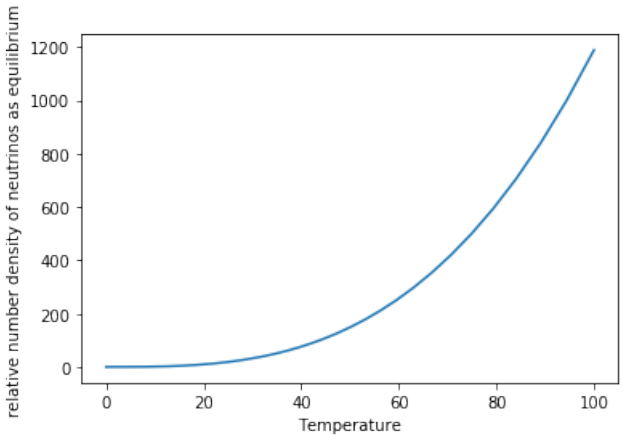

Figure 4.1: The neutrino density in the universe

The computational integration technique used was a pre-built Scipy function *quad*. This integration function computed a definite integral with set bounds using a numerical quadrature method. This method operates by choosing an initial 'abscissas' where the chosen function is evaluated at, this is repeated many times (with many other intermediate steps, not necessary to outline here) and a weighting of each abscissas is determined through the use of a Lagrange interpolating polynomial. The final output is the integral of the function between the chosen boundaries and the error on that value.
The density of neutrinos in the early universe as a function of temperature was determined using the integration method outlined above. The relative density of neutrinos within the universe as a function of time can be determined through the integration of the Friedman equation. Figure 4.1 shows this abundance increasing with temperature, as expected.
As the temperature increases so do the opportunities for particles to collide and interact resulting in decays. As

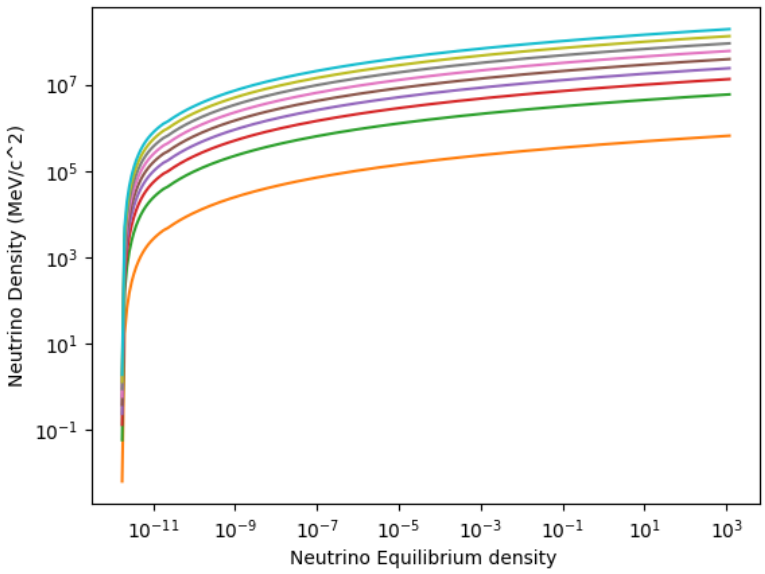

Figure 4.2: The neutrino equilibrium density as a function of Temperature. THe different colours represent a different neutrino mass between $10^{-3} MeV$

the temperature increases, so does the presence of neutrinos. To further confirm the chosen temperatures, using the Friedman equations a formula relating the Temperature to time was derived using the equations stated above. This was then numerically evaluated for a range of times to observe the evolution of the temperature of the universe over time. As we approach to the current day the temperature of the universe has significantly decreased. Therefore in order to place limits on the mass of the neutrino the temperatures present in the early universe should be used. By comparing these neutrino mass values to the observed neutrino densities appropriate limits on the mass can be placed. Current limits on the neutrino mass using similar methods to

those outlined about have placed the mass to be $\sum m_\nu < 0.17eV$ at 95% confidence (Couchot et al. 2017). This is the total mass of all the flavour types of neutrinos. The actual mass of the electron neutrino is much smaller than this, how much smaller? We are still looking.

Chapter 5

Conclusion

Through various numerical methods the mass of the electron neutrino has had very stringent limits placed upon it. Experimental methods place the neutrino mass to be around 1 MeV with large error, the Monte Carlo simulations further narrow this value down through the simulation of a neutrino beam. The more energetic, and therefore heavier mass neutrinos hit the plate further away from the centre of the detector plate. The most constraining of these methods was the use of the cosmic microwave background (CMB). By using the information about the early universe that is encoded in the background limits on the total mass of the neutrino flavours have been found. Current limits have found this neutrino mass to be $\sum m_\nu < 0.17eV$ at 95% confidence (Couchot et al. 2017).
This exercise in using a programming language to determine a physical parameter shows the possibilities and potential of scientific computation to produce fundamental science. Coupled with an easy to use graphic interface, such as jupyter notebook, these complex physical processes can be made easier to understand by the layperson and make fun science accessible to all.

Appendix A

Extension

As an extension I propose that I write an Ipython Notebook that uses the code that I have written and acts as a tutorial so that anyone else who wishes to do the experiment can just use the notebook instead of writing their own code. This would require me to use Markdown language and make the code extremely useful, well documented and versatile so that anyone can just upload their data and generate the plots that they want to. The notebook would include all of the code written for the project and be able to be run without any additional installs or steps beyond the basic python functionality.
If this were the extension I would be able to improve my code writing and documentation skills while also learning proper Markdown and Ipython Notebooks.

The knowledge of Markdown language can be very useful across a variety of situations and disciplines. Markdown can be used to create websites, educational tools and make scientific papers and journals more visually appealing. In conjunction with Ipython, Markdown can create tools that are intuitive and easy to use while also allowing the user to explore a range of complex details and code with as much or as little experience as possible.

Appendix B

```
def plot(fitshow=True, linfit=True, Errorbar=True):
    '''
    Plots the calculated data with the linear fit and error bars
    fitshow - plot the data
    linfit - plot the least squares fit
    Errorbar - plot the error
    '''
    plt.plot(x,y, label = 'data')
    if linfit:
        # Plot the data with the linear fit
        print('Plotting the least squares fit...')
        plt.plot(x, linear(x, m, c), label = 'fit')
    if Errorbar:
        print('Plotting the calculated 1 sigma variance...')
        plt.errorbar(x, linear(x,m,c), yErrArray, xErrArray,
        ecolor = 'lightgrey', color = 'o', ls = '', label = '1 STD error')
    plt.xlabel('Kinetic Energy keV')
    plt.ylabel('KurieVar')
    plt.title('Kurie Plot')
    plt.legend()
    plt.show()
```

Figure B.1: The code used to generate the Kurie Plot in Python3

Bibliography

[1] ArgoNeuT Collaboration et al. "First measurement of the cross section for ν_μ and $\bar{\nu}\_\mu$ induced single charged pion production on argon using ArgoNeuT". In: *ArXiv e-prints* (Apr. 2018). arXiv: 1804.10294 [hep-ex].

[2] H. Bethe and R. Peierls. "The Neutrino". In: 133 (Apr. 1934), 532. doi:10.1038/133532a0.

[3] S. M. Bilenky. "Neutrino. History of a unique particle". In: *European Physical Journal H* 38 (May 2013), 345–404. doi:10.1140/epjh/e2012-20068-9. arXiv: 1210.3065 [hep-ph].

[4] F. Couchot et al. "Cosmological constraints on the neutrino mass including systematic uncertainties". In: 606, A104 (Oct. 2017), A104. doi:10.1051/0004-6361/201730927. arXiv: 1703.10829.

[5] G.-y. Huang, T. Ohlsson, and S. Zhou. "Observational constraints on secret neutrino interactions from big bang nucleosynthesis". In: 97.7, 075009 (Apr. 2018), 075009. doi:10.1103/PhysRevD.97.075009. arXiv: 1712.04792 [hep-ph].

[6] S. Mertens. "Direct Neutrino Mass Experiments". In: *Journal of Physics Conference Series*. Vol. 718. Journal of Physics Conference Series. May 2016, 022013. doi:10.1088/1742-6596/718/2/022013. arXiv: 1605.01579 [nucl-ex].

[7] N. Palanque-Delabrouille et al. "Neutrino masses and cosmology with Lyman-alpha forest power spectrum". In: 11, 011 (Nov. 2015), 011. doi:10.1088/1475-7516/2015/11/011. arXiv: 1506.05976.

[8] Frederick Reines and Clyde L. Cowan. "Free Antineutrino Absorption Cross Section. I. Measurement of the Free Antineutrino Absorption Cross Section by Protons". In: *Phys. Rev.* 113 (1 1959), 273–279. doi:10.1103/PhysRev.113.273. https://link.aps.org/doi/10.1103/PhysRev.113.273.

[9] University of Zurich, *Standard Model*. Available at http://www.physik.uzh.ch/en/researcharea/lhcb/outreach/StandardModel.html (2018/04/25). 2018.

[10] M. Zennaro et al. "Cosmological constraints from galaxy clustering in the presence of massive neutrinos". In: 477 (June 2018), 491–506. doi:10.1093/mnras/sty670. arXiv: 1712.02886.